Photochemical & Photobiological Sciences

PAPER

Cite this: *Photochem. Photobiol. Sci.*, 2018, **17**, 741

Nanosecond laser flash photolysis of a 6-nitroindolinospiropyran in solution and in nanocrystalline suspension under single excitation conditions†

Vanessa M. Breslin,[a] Nicole A. Barbour,[a] Duy-Khoi Dang,[b] Steven A. Lopez [b] and Miguel A. Garcia-Garibay *[a]

Received 3rd March 2018,
Accepted 9th May 2018

DOI: 10.1039/c8pp00095f

rsc.li/pps

Nanosecond transient absorption spectroscopy was used to study the photochemical ring-opening reaction for a 6-nitroindolinospiropyran (**SP1**) in solution and in nanocrystalline (NC) suspension at 298 K. We measured the kinetics in argon purged and air saturated acetonitrile and found that the presence of oxygen affected two out of the three components of the kinetic decay at 440 nm. These are assigned to the triplet excited states of the *Z*- and *E*-merocyanines (^{3}***Z*-MC***** and ^{3}***E*-MC***). In contrast, a long-lived growth component at 550 nm and the decay of a band centered at 590 nm showed no dependence on oxygen and are assigned, respectively, to the ground state *Z*- and *E*-merocyanines (***Z*-MC$_0$** and ***E*-MC$_0$**). Laser flash photolysis studies performed in NC suspensions initially showed a very broad, featureless absorption spectrum that decayed uniformly for *ca.* 70 ns before revealing a more defined spectrum that persisted for greater than 4 ms and is consistent with a mixture of the more stable ***Z*-** and ***E*-MC$_0$** structures. We performed quantum mechanical calculations on the interconversion of ***E*-** and ***Z*-MC**s on the **S$_0$** and **S$_1$** potential energy surfaces. The computed UV-vis spectra for a scan along the *Z* → *E* interconversion reaction coordinate show substantial absorptivity from 300–600 nm, which suggests that the broad, featureless transient absorption spectrum results from the contribution of the transition structure and other high-energy species during the *Z* to *E* isomerization.

Introduction

The photochromic reaction of the spiropyran-merocyanine system (**SP-MC**, Scheme 1) has been studied extensively in solution and polymer matrices.[1–5] However, fewer reports exist that describe the crystalline state photochromism of these compounds,[6–9] which have applications as molecular switches due to their ability to respond to a variety of stimuli such as light, solvent polarity, pressure, temperature, and pH.[1,2,4,10–14] Scheme 1 shows the photochromic reaction for the 6-nitroindolinospiropyran (**SP1**) studied in this work with UV light irradiation causing the cleavage of the C_{spiro}–O bond to produce the colored ***Z*-** and ***E*-MC** ring-opened isomers. The

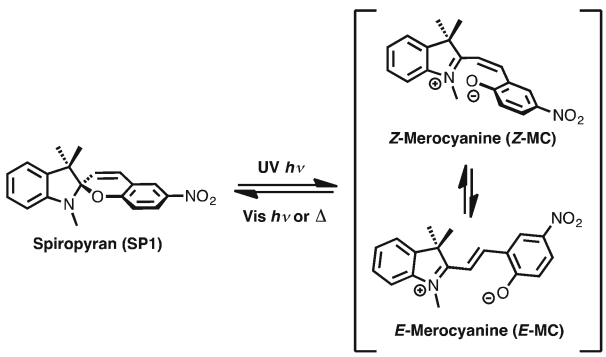

Scheme 1

MC species can then return back to the spiro form either thermally or photochemically.

Although the photochromism of spiropyrans is generally well-documented in solution and more recently in crystals, the photochemical mechanism for the **SP** → **MC** ring-opening process remains a source of some debate.[15–17] While nanosecond, picosecond, and even femtosecond laser flash photo-

[a]*Department of Chemistry and Biochemistry, University of California, Los Angeles, California 90095, USA. E-mail: mgg@chem.ucla.edu*
[b]*Department of Chemistry and Chemical Biology, Northeastern University, Boston, Massachusetts 02115, USA*

†Electronic supplementary information (ESI) available: Photochemical procedures, UV-vis spectra, PXRD and DLS nanocrystal data, laser flash photolysis kinetic plots in acetonitrile, computational methods, and calculated energies for ***E*-** and ***Z*-MC**s. See DOI: 10.1039/c8pp00095f

lysis have been used in elucidating the photochemical mechanism of **SP**s in solution, polymer films, and crystalline solids, different interpretations of the similar spectral and kinetic data have been reported.[10,15,16,18–26] Several reasons may account for the different suggestions, including the spectral overlap of multiple transient species, the potential involvement of side reactions, and differences in experimental conditions.[15]

For example, in a study carried out in hexane solution by Lenoble *et al.*,[16] a transient absorption band at 630 nm was assigned to a merocyanine dimer species. A similar study reported by Krysanov and Alfimov in benzene did not describe any absorption bands maximizing above 600 nm, suggesting that dimers were not produced in their experiments.[27] Subsequent studies based on these observations found that dimer complexes or higher aggregates involving **SP** and **MC** species would be preferentially formed in saturated aliphatic hydrocarbons with more concentrated samples resulting in more aggregate formation upon irradiation.[28–30] Variations in the reported excited state kinetic data have also resulted in different species being assigned to the transient observed between 420–450 nm in almost every kinetic study involving nitro-substituted spiropyrans, such as **SP1**.[10,15–18,28] These discrepancies and our interest in exploring the reaction in the solid state have served as motivation for our present work. Here we intend to shed more light on the mechanism for the photochemical ring-opening of **SP1** in solution and the crystalline state. A key aspect of our investigation in the solid state is the use of transient absorption analysis using nanosecond pump–probe spectroscopy with nanocrystals (NC) suspended in water. Nanocrystals that are smaller than the wavelength of incident light make it possible to use conventional transmission methods by diminishing complications that arise from dichroism, birefringence, and light scattering.[31] An additional advantage of paramount importance for this work, which has been shown in previous studies,[32–34] is that suspended nanocrystals make it possible to study photochemical reactions under single excitation conditions, thus avoiding multiphotonic processes that are commonly observed in bulk solids.[35] We are therefore interested in using NC suspensions to study how the nanocrystal environment affects the kinetics of photochemical reactions in order to compare to solution and bulk solid studies.

In fact, a limited number of studies describing the photochromic reaction of spiropyrans and spirooxazines in crystals using pulsed laser excitation have been reported, with the majority being described by Masuhara and coworkers.[22–26] In their first study, they showed that weak laser excitation (<1 mJ cm^{-2}) of their spirooxazine microcrystalline powders never resulted in the color changes indicative of a stable merocyanine species.[23] However, increasing the laser intensity to a few mJ cm^{-2} resulted in the expected coloration of the powder samples, which was attributed to the formation of an ***E*-MC** species (Scheme 1). They suggested that the excess light energy not used to break the C_{spiro}–O bond would still be absorbed by the crystal as heat and would result in rapid local heating, which could produce enough flexibility in the crystal lattice to allow for the formation of a stable ***E*-MC**. However, it is also possible that their observations were the result of multiphotonic interactions from the intense excitation pulses. They then went on to perform "double pulse excitation" experiments, which involved using a half mirror to divide a femtosecond excitation pulse into two, and then reintroducing the two pulses to the sample with an optical delay varied from 40 ps to 5 ns.[25] The laser fluence of each pulse was held constant at 1.7 mJ cm^{-2}. The authors found that when the time interval between the two pulses was less than 3 ns the observed **MC** absorption at *ca.* 600 nm was greater than that observed in the single pulse experiments at the same laser fluence of 1.7 mJ cm^{-2}, whereas at delays greater than 3 ns the observed **MC** absorption was the same as that in the single pulse experiments. This suggested that the photoprocesses induced by the first pulse are correlated to those induced by the second pulse at short delay times (<3 ns) and not correlated at longer delay times (>3 ns). The authors noted that these results, however, cannot be well explained by the photothermal model described above where local heating of a crystal from laser excitation can induce enough lattice disorder to allow the ***E*-MC** to form. This is because thermal diffusion is estimated to occur on the microsecond time scale, meaning that the amount of **MC** produced between two excitation pulses separated by delays of more than 10 ns should still be correlated, which is not what the double pulse experimental data shows. Therefore, Masuhara and coworkers proposed a new model, which they call the cooperative photochemical reaction model. In this model, the authors suggest that intense pulsed laser excitation should produce a high density of ***Z*-MC** excited states, resulting in the sites containing multiple transient species having enough local lattice disorder to create the free volume necessary for isomerization to a long-lived planar ***E*-MC** to occur. Consequently, the number of lattice sites containing plural transient species at shorter delay times (<3 ns) between pulses increases with the laser fluence to produce a greater number of ***E*-MC** species and results in a greater **MC** absorbance. Additional studies by the same group found similar results for spiropyrans in microcrystalline powders as well.[22,24]

Although Masuhara and coworkers[22–26] reported that they did not observe any photocoloration of their microcrystalline powders of spiropyrans or spirooxazines with weak laser excitation or steady-state irradiation, we and others have shown that weak, continuous light sources work well,[1,6–9,13,36,37] perhaps highlighting the intensity-dependence of the photochromic reaction. Our previous work focused on the thermal decay kinetics for a set of structurally analogous nitro-substituted spiropyrans in solution and in the solid state.[1] Specifically, we used nanocrystals suspended in water to study the solid state photochromism of spiropyrans using transmission spectroscopy.[1] We showed that a set of five *N*-alkyl substituted 6-nitroindolinospiropyrans underwent rapid coloration with thermal recovery kinetics that are very similar in solution but varied widely in the crystalline state. Based on that study, and knowing that large single crystals and dry

powders can exhibit complex kinetics as a result of multiphotonic interactions, we have shown that NC suspensions can be used to explore absolute kinetics in the solid state.[38–41] Here we compare the excited state ring-opening reaction for a 6-nitroindolinospiropyran (**SP1**) in solution and in NC suspension using nanosecond transient absorption spectroscopy. Specifically, we set out to study how the nanocrystal environment affects the kinetics of the photoreaction of **SP1** upon pulsed laser excitation. By choosing conditions known to disfavor dimer and aggregate formation in solution, we identified what we hypothesize to be the *E* and *Z* ground state merocyanine species and also propose the presence of a triplet excited state species whose identity will be discussed in the next section. Our results in NC suspension showed a very broad transient spectrum immediately after the laser pulse, which after about 70 ns transforms into the spectrum of a long-lived **MC** isomer, suggesting that spiropyrans in NCs behave more similarly to **SP**s in solution than they do to **SP**s in microcrystalline powders.

Experimental

Synthesis of SP1

SP1 was synthesized as previously reported in a single step from the condensation of commercially available 1,3,3-trimethyl-2-methyleneindoline with 2-hydroxy-5-nitrobenzaldehyde.[1]

Solution sample preparation

730 μL of a stock solution (17.2 mM) of **SP1** in acetonitrile was diluted to 500 mL to give a final sample concentration of 0.025 mM with an optical density of *ca.* 0.25 at 355 nm.

NC suspension sample preparation

15 μL of a stock solution (~50 mM) of **SP1** in acetonitrile was injected *via* a micropipette into a graduated cylinder containing a vigorously stirring solution of 16 mL of Millipore water and 4 mL of an aqueous CTAB (cetyltrimethylammonium bromide) solution (0.193 mM). The vigorous stirring was continued for 30 seconds after injection. The newly created suspension was gently poured into a large culture tube and sonicated for 2 minutes. The suspension was then immediately used for LFP studies and new suspensions were made as needed. NC suspensions had an optical density of *ca.* 0.365 at 355 nm.

Transient absorption measurements

Nanosecond laser flash photolysis experiments were performed using a Brilliant b Quantel Q-switched Nd:YAG laser operating at 355 nm with a repetition rate of 1 Hz and a pulse width of *ca.* 8 ns. Samples were flowed continuously through a 1 cm quartz flow cell mounted on a home-built sample holder with all measurements carried out in single pass experiments. Degassed solutions were purged with argon for 3 hours prior to and throughout the course of the transient absorption experiments. Air saturated solutions were allowed to equilibrate overnight under standard atmospheric conditions prior to transient absorption experiments.

Results and discussion

Sample characterization and flash photolysis setup

In order to study the transient kinetics of **SP1** *via* laser flash photolysis, we prepared and analyzed the stability of **SP1** in acetonitrile solutions (0.025 mM) and aqueous nanocrystalline (NC) suspensions (ESI, Fig. S1 and S2†). NC suspensions of **SP1** were prepared by the solvent shift, or reprecipitation method,[42] and their crystallinity was established by powder X-ray diffraction (PXRD) (ESI, Fig. S3†). Although the presence of small amounts of amorphous materials cannot be rigorously excluded, we assume that our observations are representative of the much greater crystalline component. Using dynamic light scattering (DLS), we determined the size of our nanocrystals averaged between 200–365 nm (ESI, Fig. S4†), which is smaller than the excitation wavelength. Under these conditions, optical effects such as scattering and birefringence are reduced as compared to those of bulk solids, thus making them amenable to transmission spectroscopy measurements.[31] UV-vis spectra were obtained for NC suspensions of **SP1**, which showed significant scattering and broader peaks compared to those collected in acetonitrile solutions (Fig. 1). However, the spectral features for **SP1** in NC suspensions are clearly visible, rendering our suspensions suitable for analysis *via* transmission spectroscopic methods.

Laser flash photolysis (LFP) spectroscopic studies of **SP1** were carried out in argon degassed and air saturated acetonitrile solutions as well as in NC suspensions. The solutions and suspensions were flowed continuously, but only once through the quartz cell, to ensure that pristine sample was available for each laser excitation pulse. All LFP data was reproduced in triplicate (see ESI† for additional spectra).

Solution photochemical studies

Fig. 2a shows how the transient absorption spectrum for **SP1** in argon degassed acetonitrile evolves over time starting

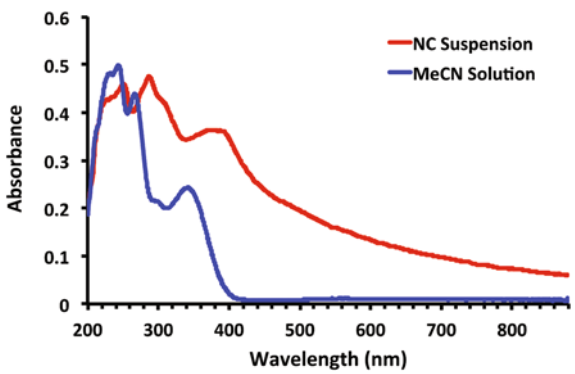

Fig. 1 UV-vis absorption spectra of **SP1** in acetonitrile (blue) and in nanocrystalline (NC) suspension (red).

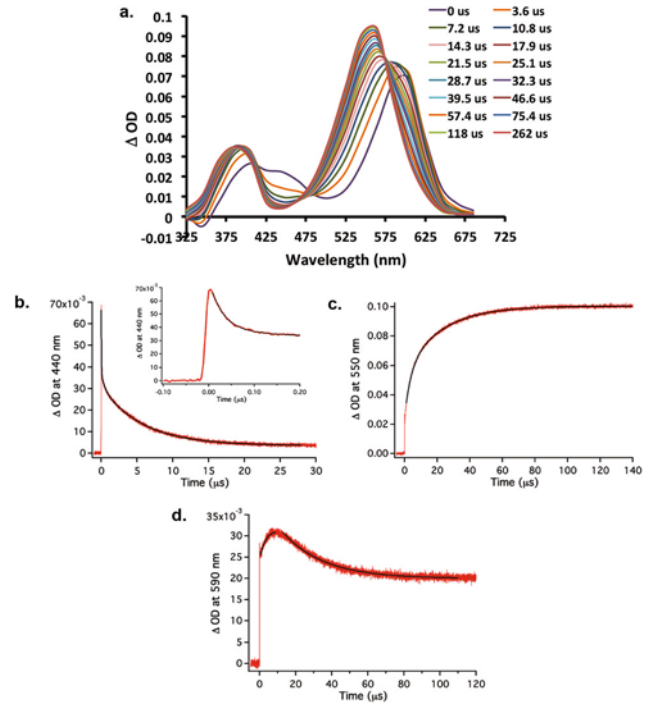

Fig. 2 (a) Transient absorption spectrum for **SP1** at various time points in argon degassed acetonitrile along with the corresponding transient kinetic plots showing (b) a decay at 440 nm, (c) a growth at 550 nm, and (d) a growth followed by a decay at 590 nm. Fit lines are shown in black.

immediately after the laser pulse (0 μs) and continuing until 262 μs after the laser pulse. The end-of-pulse spectrum is characterized by three absorption bands with maxima at 410, 440, and 590 nm. Over time, the band at 440 nm decays while the bands at 410 and 590 nm appear to undergo a growth and shift to 380 and 550 nm, respectively. While these multiple absorption bands are known in the literature, the identities and kinetics for the absorbing species are ambiguous.[15,16,18–21] To address that, we collected kinetic data at the different absorption maxima identified in Fig. 2a for an argon degassed sample of **SP1** in acetonitrile. The kinetic data obtained at 440 nm revealed three decay components with lifetimes of 31 ns, 495 ns, and 5.7 μs (Fig. 2b). Subsequent analysis of the absorption at 590 nm showed a very rapid growth within the laser pulse (lifetime could not be measured) with a slower monoexponential growth component of 2.9 μs followed by a monoexponential decay of 22.9 μs (Fig. 2d). Finally, the kinetic data collected at 550 nm also revealed a very rapid growth within the laser pulse (lifetime could not be measured) followed by a biexponential growth with lifetimes of 3.1 μs and 22.0 μs (Fig. 2c). The absorption bands observed at 380 and 410 nm were found to have the same transient kinetics as those at 550 and 590 nm, respectively, which suggests that one transient species absorbs at both 380 and 550 nm and another at 410 and 590 nm. In the work of Lenoble and Becker, very similar transient absorptions at 370, 430, 530, and 570 nm were identified for solutions of **SP1** in hexane.[16] Specifically, they assigned the absorptions at 370 and 570 nm to a single species, namely the ***E*-MC**. Another report by Görner states that the ***E***- and ***Z*-MC** ground state isomers both have absorptions between 390–410 nm and 560–620 nm,[10] which supports our experimental observations.

In order to compare the different transient species we observed upon the excitation of **SP1** in argon degassed acetonitrile to literature assignments, we gathered a similar transient absorption spectrum of **SP1** in air saturated acetonitrile to establish the effects of oxygen as a triplet quencher. Fig. 3a shows how the transient absorption spectrum for **SP1** in air saturated acetonitrile evolves over time starting immediately after the laser pulse (0 ns) and continuing until 3.49 μs after the laser pulse. The end-of-pulse spectrum is characterized by two absorption bands with maxima at 430 and 590 nm. Over time, the band at 430 nm decays and splits into two bands with maxima at 410 and 440 nm, which then follow the same spectral progression seen in Fig. 2a for the argon degassed sample. The bands at 410 and 590 nm appear to undergo a similar growth and shift to 380 and 550 nm, respectively, just as in the argon degassed sample. However, several transient lifetimes were found to be different. The kinetic data obtained at 440 nm revealed a biexponential decay with lifetimes of 24 ns and 186 ns (Fig. 3b), which is different than the three component decay observed at 440 nm in the argon degassed sample. The short decay component in both cases is very similar (31 and 24 ns), suggesting that this transient is too short-lived to interact with and be quenched by oxygen.

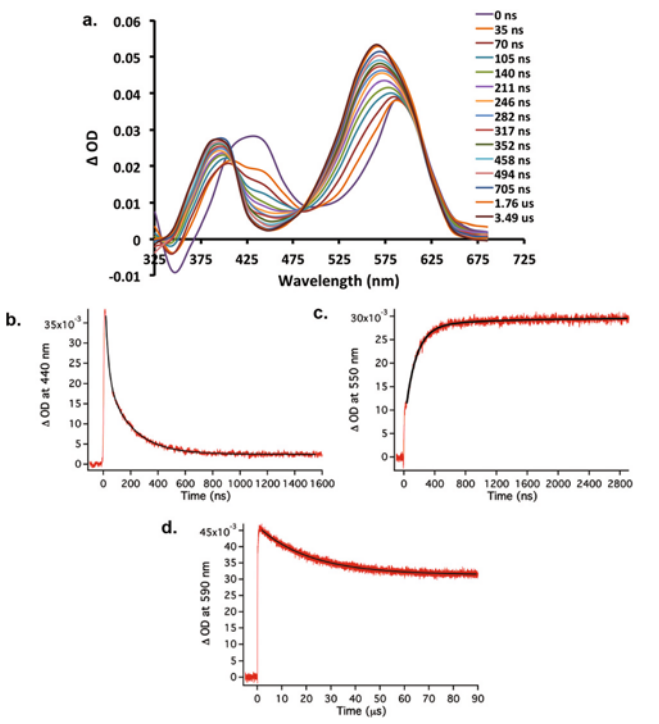

Fig. 3 (a) Transient absorption spectrum for **SP1** at various time points in air saturated acetonitrile along with the corresponding transient kinetic plots showing (b) a decay at 440 nm, (c) a growth at 550 nm, and (d) a decay at 590 nm. Fit lines are shown in black.

However, only one other transient lifetime is found in air saturated acetonitrile, compared to two in argon degassed solution, which implies that oxygen only partially quenches one of the transients (495 to 186 ns) and completely quenches the longest-lived transient (5.7 μs to 0 ns). This data suggests that multiple transients absorb at 440 nm with at least one of them being a triplet species due to the presence of oxygen affecting some of the lifetimes. Continuing our data analysis, the kinetics at 590 nm revealed one very rapid growth within the laser pulse, for which a lifetime could not be calculated, followed by a monoexponential decay with a lifetime of 21.5 μs (Fig. 3d). The kinetics at 550 nm showed an initial growth within the laser pulse followed by a biexponential growth with lifetimes of 156 ns and 20.4 μs (Fig. 3c). The decay lifetime at 590 nm remains essentially constant both in the presence and absence of oxygen. This suggests that the absorbing species is not a triplet, but rather a ground state. The same can be said of the longer-lived portion of the kinetic growth at 550 nm, implying that this species is also a ground state. A final observation we made concerning our solution transient data (argon degassed and air saturated) is that the decays at 440 and 590 nm never return to the original baseline value, as others have also observed.[10,15,16,18] The reason for this is most likely due to the fact that the long-lived species at 550 nm absorbs at both of these wavelengths, and thus makes it appear as if the transients at 440 and 590 nm have an extremely long-lived component of their own or decompose.

Mechanistic analysis

With our transient kinetic results in solution now in hand, we can put our data in the context of a photochemical mechanism from spiropyran to merocyanine. Our proposed mechanism is shown in Scheme 2 with observable transient species shown between braces and their absorbance maxima indicated below, with the final product being ***E*-MC$_0$**. For nitro-substituted spiropyrans such as **SP1**, it has been established that UV irradiation excites the ground state spiropyran (**SP$_0$**) to its first excited singlet state (^{1}**SP***), which then intersystem crosses (ISC) to the excited triplet state (^{3}**SP***).[15,16,43–45] The ^{3}**SP*** then undergoes rapid ring-opening to a triplet merocyanine species, the identity of which the literature still does not agree on. What the literature does agree on is that the photochemical processes just mentioned occur on a sub-nanosecond time scale, which is shorter than our laser pulse, such that our analysis begins with the triplet merocyanine species (^{3}***Z*-MC***). The

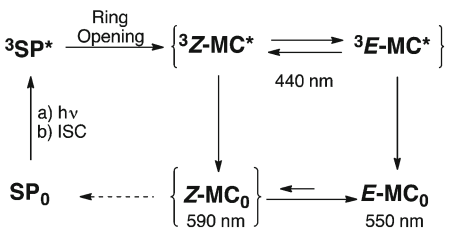

Scheme 2

decay we measured at 440 nm has previously been assigned to several different triplet species, such as the triplet spiropyran (^{3}**SP***),[17,28] triplet *Z*-merocyanine (^{3}***Z*-MC***),[16] the triplet *E*-merocyanine (^{3}***E*-MC***),[15,18] or a somewhat ambiguous triplet perpendicular merocyanine conformer (^{3}**perp***),[10,15,18] which is described as a merocyanine isomer that maintains the same orthogonal orientation of its two ring systems as in the spiropyran form. We propose that the band at 440 nm includes overlapping absorptions for both ^{3}***Z*-MC*** and ^{3}***E*-MC***. In fact, the experimentally determined decay lifetimes do not correlate with any of the growth lifetimes at 550 or 590 nm, meaning that the true kinetics at 440 nm are obscured by having multiple species with different extinction coefficients absorbing in the same region. Although the ^{3}**perp*** has been proposed previously as the species that gives rise to the absorption at 440 nm, calculations discussed below suggest that the ^{3}**perp*** species should be considered more like a transition state between the ^{3}***E*-** and ^{3}***Z*-MC*** species, and therefore may not be an observable transient species in solution. As for the possibility that the ^{3}**SP*** is the triplet species absorbing at 440 nm, Chibisov and Görner observed a transient at 440 nm with a decay lifetime in the microsecond time domain.[15,18] However, in oxygen saturated solution, the decay at 440 nm was almost completely quenched. If we make the assumption that ^{3}**SP*** is long-lived enough and efficiently populated at room temperature, then quenching by oxygen should result in ISC to the **SP$_0$** with almost no ***Z*-** or ***E*-MC$_0$** being produced. Since their experimental evidence shows significant ***Z*-** and ***E*-MC$_0$** formation in both argon and oxygen saturated solutions just as we observe in argon degassed and air saturated solutions, this suggests that the ^{3}**SP*** is too short-lived to interact with and be quenched by oxygen, which is why we do not assign our transient at 440 nm to the ^{3}**SP***. Chibisov and Görner have also determined the rate constants for triplet quenching by oxygen in several solvents, which ranged between 0.5–2 × 10^9 M^{-1} s^{-1} and gives a benchmark for how fast the spiropyran ring-opening occurs.[18,46]

Turning our attention now to the absorption bands at 550 and 590 nm, previous reports have described them as either one broad absorption from 500–650 nm or as one absorption band with a maximum at 570 nm and a shoulder at 630 nm, and assigned them as a mixture of the *E* and *Z* ground state merocyanine species (***E*/*Z*-MC$_0$**).[16,18–20] Our results in argon degassed acetonitrile (Fig. 2a) show two absorption bands that appear to evolve from one to the other with no clear isosbestic point, suggesting a combination of spectral relaxation and equilibration. From Fig. 3 (in air saturated acetonitrile) we found that as the absorption band at 590 nm decreases with a lifetime of 21.5 μs, the long-lived portion of the growth at 550 nm has a lifetime of 20.4 μs. Since these long lifetimes are quite similar to those observed in argon degassed solution, we propose that these transients are not affected by oxygen, meaning that neither of these bands correspond to a triplet species. From the transient absorption spectra in Fig. 2a and 3a, we observe an apparent shift from 590 nm to 550 nm, which we measured as a decay at 590 nm and a growth at

550 nm. In our previous steady-state solution studies we found that the ***E*-MC$_0$** absorbs at *ca.* 550 nm in acetonitrile,[1] and so we assign the band at 590 nm to the ***Z*-MC$_0$** and the one at 550 nm to the ***E*-MC$_0$**. The ***E***- and ***Z*-MC$_0$** are shown in Scheme 2 to be in an equilibrium that favors ***E*-MC$_0$**, which is in agreement with previous steady-state studies involving the **SP-MC** system.[1,2,11,47–49]

DFT calculations also support our ***E*/*Z*-MC$_0$** assignments as the $S_0 \rightarrow S_1$ 0–0 transition energy (E_{0-0}) computed for the ***Z*-MC** is lower than that for the ***E*-MC**, which is consistent with our experimental observation of the ***E*-MC$_0$** being blue-shifted relative to the ***Z*-MC$_0$** (Fig. 4). These computations were performed at the CAM-B3LYP-(D3BJ)/6-311++G(d,p)[50–53] IEFPCM-(CH_3CN) level of theory with time-dependent (TD) considerations for the excited states in Gaussian 16.[54] Additionally, our computational methods were able to predict that the ***E*-MC** has a higher absorptivity than does the ***Z*-MC** (ESI, Fig. S13†), as observed in our solution experiments (Fig. 2a).

Using our suggested assignments for the observed transient absorption bands, we can interpret the rest of our kinetic data to complete our proposed mechanism from ^{3}***E*-MC*** and ^{3}***Z*-MC*** to ***E*-MC$_0$** and ***Z*-MC$_0$**. The kinetic growth we observe at 590 nm has a lifetime of 2.9 μs in argon degassed acetonitrile, but in air saturated acetonitrile this growth appears to be contained within the laser pulse and so the kinetics could not be measured with our nanosecond laser system. Since this lifetime is affected by the presence of oxygen, it implies that a triplet species immediately precedes the ***Z*-MC$_0$** along the photochemical pathway. The same observation was made with the short-lived portion of the kinetic growth at 550 nm, which had a lifetime of 3.1 μs in argon degassed acetonitrile and a much shorter lifetime of 156 ns in air saturated acetonitrile, thus indicating that a triplet state immediately precedes the ***E*-MC$_0$** as well. With the kinetic growth lifetimes at 550 and 590 nm being essentially identical in argon degassed and air saturated acetonitrile, we postulate that either the same triplet species, *i.e.* the ^{3}***E*-MC*** or ^{3}***Z*-MC***, could be responsible for populating both the ***E***- and ***Z*-MC** ground states, or the ^{3}***E*-MC*** and ^{3}***Z*-MC*** could be in rapid equilibrium with each other and then decay with similar rates to their respective ground states. Others have argued that the ^{3}***E*-MC*** does not directly intersystem cross to the ***E*-MC$_0$** because only fluorescence, not phosphorescence, was observed upon excitation of the ***E*-MC$_0$** to the ^{1}***E*-MC*** in acetonitrile.[10,18] However, this argument is questionable as it compares two different mechanisms to access the ^{3}***E*-MC***.

Solid state photochemical studies

With a detailed investigation of the nanosecond transient kinetics of **SP1** in acetonitrile experimentally characterized, we began studying the same spiropyran model in the solid state. As mentioned in the introduction, we chose to use aqueous nanocrystalline suspensions in order to increase the probability of observing single excitation photoprocesses. Regarding the excitation of our nanocrystals, the power of our laser (*ca.* 8×10^6 W) is three to four orders of magnitude smaller than the one used by Masuhara and coworkers[22] (*ca.* 3×10^9–2×10^{10} W), which supports our expectation that the signals observed upon laser flash photolysis of **SP1** in NC suspension are more likely the result of single excitation events. Fig. 5 shows the transient absorption spectrum for an NC suspension of **SP1** from 0–310 ns, with the bottom portion expanded from 78–310 ns. The observed spectrum can be described as very broad, featureless, and appears to decay uniformly over all wavelengths from 325–675 nm with a maximum near 330 nm. However, the expanded bottom portion of the spectrum shows some spectral definition with two noisy

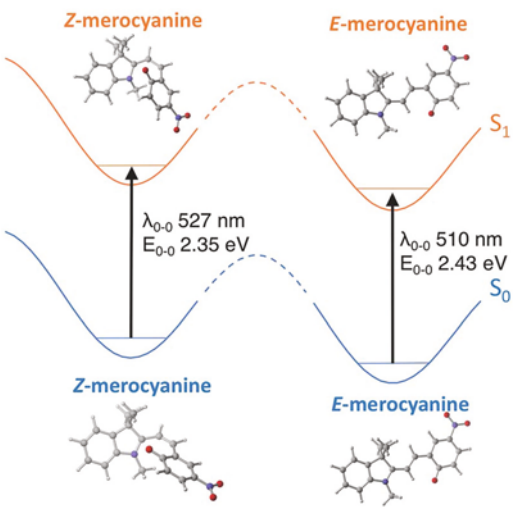

Fig. 4 Calculated 0–0 transitions for the ***Z***- and ***E*-MC** from $S_0 \rightarrow S_1$ with transition energies provided in nm and eV following a procedure reported by Adamo and Jacquemin[55] using (TD)-CAM-B3LYP-(D3BJ)/6-311++G(d,p) IEFPCM-(CH_3CN).

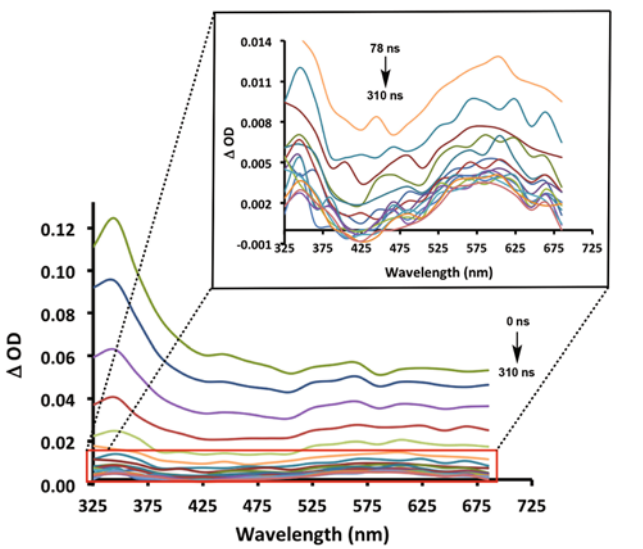

Fig. 5 Transient absorption spectrum for **SP1** at various time points in NC suspension. Red box: expansion of spectrum at longer times. Laser output (λ = 355 nm, 36–40 mJ per pulse, 5–8 ns, 10 Hz).

absorptions, one below 400 nm and the other between 500–685 nm, which looks similar to the final absorption spectrum for **SP1** in solution under both argon degassed and air saturated conditions (Fig. 2a and 3a), suggesting that both ***E***- and ***Z***-like $\mathbf{MC_0}$ isomers are produced in NC suspension.

To analyze our results, we recall that Masuhara and coworkers have described the solid state transient kinetics of **SP1** in microcrystalline powders and PMMA films using a femtosecond diffuse reflectance experimental setup.[22] An observation they made was that the growth they observed between 550–650 nm with a maximum at *ca.* 630 nm was assigned to a merocyanine species in both microcrystalline powders and PMMA films and that it reached its maximum absorption after *ca.* 5 ns. However, in the powder sample they found that this species decayed biexponentially with lifetimes of 20 and 150 μs, whereas in the PMMA films the decay of this absorption was shown to take several tens of minutes.[22] In agreement with our previous steady state excitation studies which revealed merocyanine lifetimes of minutes to hours,[1] we do not observe a decay of the transient absorption band between 550–650 nm in our NC suspensions at timescales up to 4 ms (Fig. 5, inset), suggesting that **SP1** is capable of attaining a stable ***E***-like **MC** configuration in the crystalline environment, even when using a weaker excitation pulse. One may consider the possibility that the original broad transient and the subsequent long-lived ***E***-like **MC** signal may be due to merocyanine formed on the surface of the nanocrystals. However, one can estimate that surface sites account for no more than *ca.* 2–3% of the total molecules in each (200–400 nm) nanocrystal. Furthermore, considering that crystals of this size are able to transmit light, it is unlikely that excitation can only occur on the surface. Therefore, we suggest that it is reasonable to conclude that **MC** molecules are mainly generated in the bulk of the nanocrystals, as it is likely that the evolution of surface transients under significantly lower constraints should approach the evolution of those observed in solution.

The extremely broad and featureless transient absorption we observe in NC suspensions using laser flash photolysis is quite different from the one in solution. Since the solid state spectrum did not resolve on the nanosecond timescale, we can only speculate as to the nature of the solid state photochemical mechanism. We start our analysis by considering that the absorption spectra of linearly conjugated chromophores tend to be highly sensitive to conformational changes that have an effect on the extent of conjugation. Based on that, it is reasonable to postulate that the broad spectrum in Fig. 5 may be the result of multiple absorbing species, rather than arising from a single chromophore that absorbs over all wavelengths. A plausible scenario involves a ring-opening reaction from ^{3}**SP*** to the *cisoid* configuration of ^{3}***Z*-MC***, where the bonds between the indoline imminium and phenolate groups begin to evolve towards the *transoid* configuration of ^{3}***E*-MC***. One may expect that the crystal lattice can slow down the kinetics of this process, such that multiple structures may co-exist along the ^{3}***E*-MC** and ^{3}***Z*-MC*** energy surface before going to the ground state chromophore. Subsequent decay of the hypothetical ^{3}***E*-MC*** and ^{3}***Z*-MC*** species to the long-lived ground state ***E*-$\mathbf{MC_0}$** would result in the more defined final spectrum in the expanded portion of Fig. 5. Since we do not observe a growth of ***Z*-$\mathbf{MC_0}$** as we do in solution, this interpretation would require that ^{3}***E*-MC*** and ^{3}***Z*-MC*** have a greater extinction coefficient than the ***E*-$\mathbf{MC_0}$**, so that the growth of the ground state **MC**s can be obscured by the absorption of the triplet species.

In order to gain qualitative support for the suggested mechanism, we calculated the absorption profiles for numerous **MC** structures along the torsional reaction coordinate between the two rings, as shown in Fig. 6. Specifically, we evaluated the torsional potential about the central C=C π bond (highlighted in green in Fig. 6) at the CAM-B3LYP/6-31+G(d,p) level of theory to explore relatively high-energy constrained structures and their absorbance properties. While the intermediate structures along the torsional potential are not local minima in solution, we propose that the solid state may sufficiently augment their lifetimes such that they may contribute to the observed absorption. Thus, we use their structures to approximate possible high-energy conformations that are trapped in the nanocrystalline environments, and consider their corresponding absorbance profiles as a qualitative representation of the breadth of absorption for their excited states. The torsional potential in Fig. 6 shows the optimized structures along the scanned coordinate between the ***Z***- and ***E*-MC** configurations at regular 20° intervals (see ESI† for complete computational results). We then performed single-point energy calculations on each structure with the TD-CAM-B3LYP/6-311++G(d,p) method to obtain vertical excitations to the $\mathbf{S_1}$ surface and predict the UV-vis absorbance spectra for each structure as shown in Fig. 7. The absorbance curves in Fig. 7 are color-coded by their structural similarity to either the ***Z*-MC** or the ***E*-MC**. *Z*-like merocyanines (θ_{dih} = 0°–90°) correspond to the yellow, orange, and red solid curves, while *E*-like merocyanines

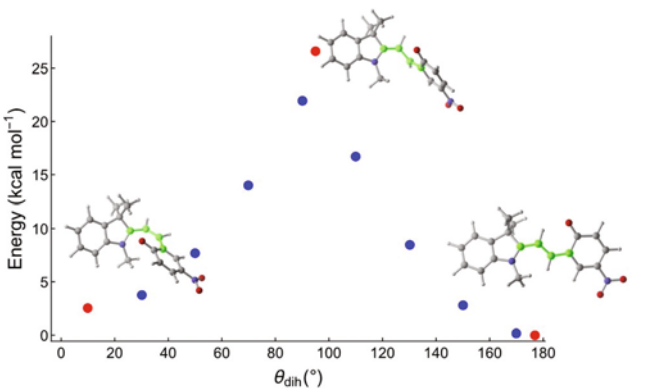

Fig. 6 Calculated energies for each geometry along the scanned coordinate based on the dihedral angle highlighted in green. Energies are relative to the optimized ***E*-MC** isomer (0 kcal mol^{-1}, θ_{dih} = 178°). The red plot points correspond to the structures shown, which are the optimized stationary points for the ***Z*-MC**, ***E*-MC**, and transition state structures. Calculations were done at the CAM-B3LYP-(D3BJ)/6-31+G(d,p) level of theory and include the IEFPCM-(CH_3CN) bulk solvation correction.

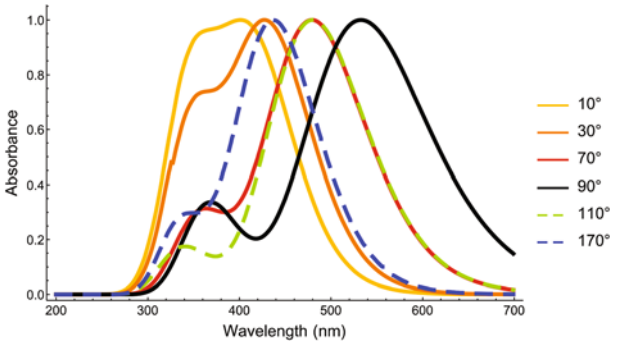

Fig. 7 The computed spectra are computed using the TD-CAM-B3LYP/6-311++G(d,p) single point energies based on the constrained optimizations using B3LYP/6-31+G(d,p). The solid black line corresponds to the structure closest to the transition state between ***Z***- and ***E***-**MC**. The yellow, orange, and red solid lines correspond to ***Z***-like **MC**s, and the green and blue dashed lines correspond to ***E***-like **MC**s.

(θ_{dih} = 90°–180°) correspond to the green and blue dashed curves. The solid black curve represents the structure closest to the transition state geometry between ***Z***-**MC** and ***E***-**MC**. The calculated UV-vis spectra in Fig. 7 for intermediate points along the ***Z***- to ***E***-**MC** reaction coordinate show significant absorptivity ranging from 300–600 nm. This suggests that the broad and featureless transient absorption spectrum initially observed in NC suspension (Fig. 5) could result from the simultaneous contribution of the ***E***- and ***Z***-**MC** with numerous ***E***- and ***Z***-like **MC** intermediate structures.

Conclusions

Using nanosecond transient absorption spectroscopy, we were able to measure the kinetics of the ***Z***-$\mathbf{MC_0}$ and the ***E***-$\mathbf{MC_0}$ in solution and suggest a model that includes the formation of the relatively stable ***E***-$\mathbf{MC_0}$ from rapid contributions of what appears to be equilibrated or spectrally overlapping ^{3}***Z***-**MC*** and ^{3}***E***-**MC*** and slower contributions from ***Z***-$\mathbf{MC_0}$, which appears to also form from the two triplet **MC**s. Subsequent studies in NC suspension revealed an initially broad, featureless transient spectrum that appeared to decay uniformly in *ca.* 70 ns before becoming a more defined spectrum that persisted for greater than 4 ms. DFT calculations support a model used to rationalize our solid state results by exploring how the absorption profiles for numerous ***E***- and ***Z***-like **MC** isomers change as a function of structure about the central C=C π bond. The predicted UV-vis absorbance profiles showed that relatively high-energy ***E***- and ***Z***-like **MC** conformers potentially accessible in the constrained environment of nanocrystals are represented by intermediate structures along the torsional potential, and have significant absorptivity over the range of 300–600 nm. This suggests that the initially broad and featureless transient absorption spectrum observed in NC suspension could be a sum of the absorbance profiles for numerous ***E***- and ***Z***-like **MC** transient structures. Eventually only the more stable ***E***-**MC** isomers persist, giving rise to the more defined spectrum observed at longer times. As we compare our steady state and transient studies with those of Masuhara and coworkers,[22–26] our results show that ring-opening of the spiropyran to relatively stable **MC** species can occur even when using a weaker excitation laser pulse than that used by Masuhara and coworkers. This leads us to propose that the differences observed between our work and Masuhara's may arise from the limited number of multiphotonic interactions that occur in nanocrystalline solids as compared to dry powders. This report also demonstrates that NC suspensions provide a simple medium for studying kinetics in solid state photochemical reactions by reducing challenges arising from optical effects and by reducing the probability of multiphotonic processes.

Conflicts of interest

The authors declare no competing financial interest.

Acknowledgements

This work was supported by NSF grant CHE1566041. S. A. L. thanks the National Science Foundation through the Extreme Science and Engineering Discovery Environment (XSEDE) computational resource (TG-CHE170074), the Discovery high performance computing cluster, and Northeastern University Department of Chemistry and Chemical Biology for financial support.

Notes and references

1 V. M. Breslin and M. A. Garcia-Garibay, *Cryst. Growth Des.*, 2017, **17**, 637–642.
2 R. Klajn, *Chem. Soc. Rev.*, 2014, **43**, 148–184.
3 J. K. Rad and A. R. Mahdavian, *J. Phys. Chem. C*, 2016, **120**, 9985–9991.
4 F. Berkovic, V. Krongauz and V. Weiss, *Chem. Rev.*, 2000, **100**, 1741–1754.
5 E. I. Balmond, B. K. Tautges, A. L. Faulkner, V. W. Or, B. M. Hodur, J. T. Shaw and A. Y. Louie, *J. Org. Chem.*, 2016, **81**, 8744–8758.
6 S. Bénard and P. Yu, *Adv. Mater.*, 2000, **12**, 48–50.
7 J. Harada, Y. Kawazoe and K. Ogawa, *Chem. Commun.*, 2010, **46**, 2593–2595.
8 O. Godsi, U. Peskin, M. Kapon, E. Natan and Y. Eichen, *Chem. Commun.*, 2001, 2132–2133.
9 P. Naumov, P. Yu and K. Sakurai, *J. Phys. Chem. A*, 2008, **112**, 5810–5814.
10 H. Görner, *Chem. Phys.*, 1997, **222**, 315–329.
11 J. T. C. Wojtyk, A. Wasey, N.-N. Xiao, P. M. Kazmaier, S. Hoz, C. Yu, R. P. Lemieux and E. Buncel, *J. Phys. Chem. A*, 2007, **111**, 2511–2516.

12 X. Meng, G. Qi, C. Zhang, K. Wang, B. Zou and Y. Ma, *Chem. Commun.*, 2015, **51**, 9320–9323.
13 P. L. Gentili, M. Nocchetti, C. Miliani and G. Favaro, *New J. Chem.*, 2004, **28**, 379–386.
14 R. Guglielmetti, 4n + 2 Systems: Spiropyrans, in *Photochromism: Molecules and Systems*, ed. H. Dürr and H. Bouas-Laurent, Elsevier, Amsterdam, 2003; p. 314.
15 H. Görner, L. S. Atabekyan and A. K. Chibisov, *Chem. Phys. Lett.*, 1996, **260**, 59–64.
16 C. Lenoble and R. S. Becker, *J. Phys. Chem.*, 1986, **90**, 62–65.
17 T. Bercovici, R. Heiligman-Rim and E. Fischer, *Mol. Photochem.*, 1969, **1**, 23–55.
18 A. K. Chibisov and H. Görner, *J. Phys. Chem. A*, 1997, **101**, 4305–4312.
19 H. Görner, *Chem. Phys. Lett.*, 1998, **282**, 381–390.
20 A.-K. Holm, O. F. Mohammed, M. Rini, E. Mukhtar, E. T. J. Nibbering and H. Fidder, *J. Phys. Chem. A*, 2005, **109**, 8962–8968.
21 A.-K. Holm, M. Rini, E. T. J. Nibbering and H. Fidder, *Chem. Phys. Lett.*, 2003, **376**, 214–219.
22 M. Suzuki, T. Asahi and H. Masuhara, *Mol. Cryst. Liq. Cryst.*, 2000, **345**, 51–56.
23 T. Asahi and H. Masuhara, *Chem. Lett.*, 1997, **26**, 1165–1166.
24 M. Suzuki, T. Asahi and H. Masuhara, *Phys. Chem. Chem. Phys.*, 2002, **4**, 185–192.
25 M. Suzuki, T. Asahi and H. Masuhara, *ChemPhysChem*, 2005, **6**, 2396–2403.
26 T. Asahi, M. Suzuki and H. Masuhara, *J. Phys. Chem. A*, 2002, **106**, 2335–2340.
27 S. A. Krysanov and M. V. Alfimov, *Chem. Phys. Lett.*, 1982, **91**, 77–80.
28 V. Krongauz, J. Kiwi and M. Grätzel, *J. Photochem.*, 1980, **13**, 89–97.
29 V. A. Barachevskii and R. E. Karpov, *High Energy Chem.*, 2007, **41**, 188–199.
30 Y. Kalisky, T. E. Orlowski and D. J. Williams, *J. Phys. Chem.*, 1983, **87**, 5333–5338.
31 E. A. Wood, *Crystals and Light: An Introduction to Optical Crystallography*, 2nd edn, Dover Publications, New York, 1977.
32 K. K. Chin, A. Natarajan, M. N. Gard, L. M. Campos, H. Shepard, E. Johansson and M. A. Garcia-Garibay, *Chem. Commun.*, 2007, 4266–4268.
33 G. Kuzmanich, S. Simoncelli, M. N. Gard, F. Spänig, B. L. Henderson, D. M. Guldi and M. A. Garcia-Garibay, *J. Am. Chem. Soc.*, 2011, **133**, 17296–17306.
34 S. Simocelli, G. Kuzmanich, M. N. Gard and M. A. Garcia-Garibay, *J. Phys. Org. Chem.*, 2010, **23**, 376–381.
35 C. E. Swenbergy and N. E. Gaecintov, in *Organic Molecular Photophysics*, ed. J. B. Birks, John Wiley & Sons, London, 1973, ch. 10, vol. 1.
36 S. Bénard and P. Yu, *Chem. Commun.*, 2000, 65–66.
37 S. Spagnoli, D. Block, E. Botzung-Appert, L. Colombier, P. L. Baldeck, A. Ibanez and A. Corval, *J. Phys. Chem. B*, 2005, **109**, 8587–8591.
38 T. S. Chung, J. H. Park and M. A. Garcia-Garibay, *J. Org. Chem.*, 2017, **82**, 12128–12133.
39 J. H. Park, M. Hughs, T. S. Chung, A. J.-L. Ayitou, V. M. Breslin and M. A. Garcia-Garibay, *J. Am. Chem. Soc.*, 2017, **139**, 13312–13317.
40 A. J.-L. Ayitou, K. Flynn, S. Jockusch, S. I. Khan and M. A. Garcia-Garibay, *J. Am. Chem. Soc.*, 2016, **138**, 2644–2648.
41 G. Kuzmanich, C. S. Vogelsberg, E. F. Maverick, J. C. Netto-Ferreira, J. C. Scaiano and M. A. Garcia-Garibay, *J. Am. Chem. Soc.*, 2012, **134**, 1115–1123.
42 H. Kasai, H. S. Nalwa, H. Oikawa, S. Okada, H. Matsuda, N. Minami, A. Kakuta, K. Ono, A. Mukoh and H. Nakanishi, *Jpn. J. Appl. Phys.*, 1992, **31**, L1132–L1134.
43 Y. Sheng, J. Leszczynski, A. A. Garcia, R. Rosario, D. Gust and J. Springer, *J. Phys. Chem. B*, 2004, **108**, 16233–16243.
44 M. Rini, A.-K. Holm, E. T. J. Nibbering and H. Fidder, *J. Am. Chem. Soc.*, 2003, **125**, 3028–3034.
45 N. P. Ernsting and T. Arthes-Engeland, *J. Phys. Chem.*, 1991, **95**, 5502–5509.
46 A. K. Chibisov and H. Görner, *J. Photochem. Photobiol., A*, 1997, **105**, 261–267.
47 J. T. C. Wojtyk, P. M. Kazmaier and E. Buncel, *Chem. Mater.*, 2001, **13**, 2547–2551.
48 F. M. Raymo, S. Giordani, A. J. P. White and D. J. Williams, *J. Org. Chem.*, 2003, **68**, 4158–4169.
49 J. T. C. Wojtyk, A. Wasey, P. M. Kazmaier, S. Hoz and E. Buncel, *J. Phys. Chem. A*, 2000, **104**, 9046–9055.
50 T. Yanai, D. P. Tew and N. C. Handy, *Chem. Phys. Lett.*, 2004, **393**, 51–57.
51 S. Miertuš, E. Scrocco and J. Tomasi, *Chem. Phys.*, 1981, **55**, 117–129.
52 G. Scalmani and M. J. Frisch, *J. Chem. Phys.*, 2010, **132**, 114110-1–114110-5.
53 S. Grimme, S. Ehrlich and L. Goerigk, *J. Comput. Chem.*, 2011, **32**, 1456–1465.
54 M. J. Frisch, G. W. Trucks, H. B. Schlegel, G. E. Scuseria, M. A. Robb, J. R. Cheeseman, G. Scalmani, V. Barone, G. A. Petersson, H. Nakatsuji, X. Li, M. Caricato, A. V. Marenich, J. Bloino, B. G. Janesko, R. Gomperts, B. Mennucci, H. P. Hratchian, J. V. Ortiz, A. F. Izmaylov, J. L. Sonnenberg, D. Williams-Young, F. Ding, F. Lipparini, F. Egidi, J. Goings, B. Peng, A. Petrone, T. Henderson, D. Ranasinghe, V. G. Zakrzewski, J. Gao, N. Rega, G. Zheng, W. Liang, M. Hada, M. Ehara, K. Toyota, R. Fukuda, J. Hasegawa, M. Ishida, T. Nakajima, Y. Honda, O. Kitao, H. Nakai, T. Vreven, K. Throssell, J. A. Montgomery Jr., J. E. Peralta, F. Ogliaro, M. J. Bearpark, J. J. Heyd, E. N. Brothers, K. N. Kudin, V. N. Staroverov, T. A. Keith, R. Kobayashi, J. Normand, K. Raghavachari, A. P. Rendell, J. C. Burant, S. S. Iyengar, J. Tomasi, M. Cossi, J. M. Millam, M. Klene, C. Adamo, R. Cammi, J. W. Ochterski, R. L. Martin, K. Morokuma, O. Farkas, J. B. Foresman and D. J. Fox, *Gaussian 16*, Gaussian, Inc., Wallingford, CT, 2016.
55 C. Adamo and D. Jacquemin, *Chem. Soc. Rev.*, 2013, **42**, 845–856.